Cancer Gene Therapy (2014) 21, 483–490

www.nature.com/cgt

ORIGINAL ARTICLE

Measles Edmonston vaccine strain derivatives have potent oncolytic activity against osteosarcoma

E Domingo-Musibay[1,2], C Allen[2], C Kurokawa[2], JJ Hardcastle[2], I Aderca[2], P Msaouel[3], A Bansal[4], H Jiang[4], TR DeGrado[4] and E Galanis[1,2]

Osteosarcoma (OS) is the most common primary bone tumor affecting children and young adults, and development of metastatic disease is associated with poor prognosis. The purpose of this study was to evaluate the antitumor efficacy of virotherapy with engineered measles virus (MV) vaccine strains in the treatment of OS. Cell lines derived from pediatric patients with OS (HOS, MG63, 143B, KHOS-312H, U2-OS and SJSA1) were infected with MV expressing green fluorescent protein (MV-GFP) and MV-expressing sodium iodide symporter (MV-NIS) strains. Viral gene expression and cytotoxicity as defined by syncytial formation, cell death and eradication of cell monolayers were demonstrated. Findings were correlated with *in vivo* efficacy in subcutaneous, orthotopic (tibial bone) and lung metastatic OS xenografts treated with the MV derivative MV-NIS via the intratumoral or intravenous route. Following treatment, we observed decrease in tumor growth of subcutaneous xenografts ($P = 0.0374$) and prolongation of survival in mice with orthotopic ($P < 0.0001$) and pulmonary metastatic OS tumors ($P = 0.0207$). Expression of the NIS transgene in MV-NIS infected tumors allowed for single photon emission computed tomography and positron emission tomography–computed tomography imaging of virus infected tumors *in vivo*. Our data support the translational potential of MV-based virotherapy approaches in the treatment of recurrent and metastatic OS.

Cancer Gene Therapy (2014) **21,** 483–490; doi:10.1038/cgt.2014.54; published online 14 November 2014

INTRODUCTION

Osteosarcoma (OS) is the most common primary bone malignancy effecting children and young adults, and comprises roughly 5% of childhood cancers and 20% of all bone tumors. Classical OS usually arises from the medullary cavity of the metaphyseal growth plates of developing long bones, areas of rapid bone growth and turnover in children and adolescents. Histologically, cells are characterized by the production of osteoid matrix, as well as complex chromosomal karyotypes.[1,2]

Despite advances in combined modality treatment including chemotherapy and surgical techniques, which result in cure in 60–75% of patients,[3] roughly one-third of young OS patients recur or develop metastatic disease or metastasis to the lungs. Long term survival for patients with metastatic disease is $< 20\%$.[4] There has been little improvement in survival during the last 20 years, and new therapeutic approaches are needed.

Oncolytic measles virus (MV) therapy is a novel therapeutic strategy for treatment of cancer.[5] Interest in this approach was triggered by observation of spontaneous regressions of leukemias and lymphomas in developing countries after infection with wild-type virus, dating back to the 1970s.[6,7] In contrast to wild type virus, MV vaccine strains are safe.[8] They have been shown to have therapeutic efficacy in several animal models and have demonstrated early evidence of biologic efficacy in human clinical trials.[9–15] MV is a negative single-stranded RNA virus, which belongs to the family of Paramyxoviridae; the virus has six genes encoding eight proteins. MV interacts with three known cellular entry receptors through its surface H glycoprotein. These receptors include the signaling lymphocyte-activating molecule predominantly found on activated B and T lymphocytes, CD46, an inhibitory complement receptor ubiquitously expressed on all human nucleated cells[16] and Nectin-4.[17] Of note vaccine strains have been adapted to preferentially enter cells via CD46 as opposed to the signaling lymphocyte-activating molecule receptor.[18,19] Furthermore, CD46 and Nectin-4 are overexpressed in tumors,[20,21] thus conferring tumor specificity. Additional advantages of this oncolytic platform include the fact that MV strains can be engineered and retargeted to different cellular receptors.[22] RNA viruses, including MV-Edmonston (MV-Edm), are potent inducers of an antiviral, interferon-mediated, response in normal tissue. As many tumor cells have defects in interferon signaling, this increases oncolytic viral selectivity for tumors.[23,24]

We hypothesized that measles virotherapy could represent a novel therapeutic direction in the treatment of refractory OS and we tested the potency of engineered MV-strains against OS lines and xenografts. In order to monitor viral propagation, a MV-Edm strain encoding the sodium iodide symporter (NIS) gene was chosen for these experiments. The NIS gene (normally expressed on follicular thyroid cells) can also be used as an imaging transgene to monitor viral infection. Expressed NIS cotransports two sodium ions and an iodide ion into cells, with sodium gradients driving cellular uptake.[25] This allows use of gamma camera, single photon emission computed tomography (SPECT), or positron emission tomography–CT (PET-CT) for *in vivo* monitoring of viral replication following administration of ^{123}I, 99mTc isotopes or F-18 tetrafluoroborate.[25–28]

[1]Medical Oncology, Mayo Clinic, Rochester, MN, USA; [2]Department of Molecular Medicine, Mayo Clinic, Rochester, MN, USA; [3]Internal Medicine, Albert Einstein College of Medicine, New York, NY, USA and [4]Department of Radiology, Mayo Clinic, Rochester, MN, USA. Correspondence: Dr E Galanis, Medical Oncology, Mayo Clinic, 200 First Street SW, Rochester, MN 55905, USA.
E-mail: galanis.evanthia@mayo.edu
Received 23 June 2014; revised 17 September 2014; accepted 18 September 2014; published online 14 November 2014

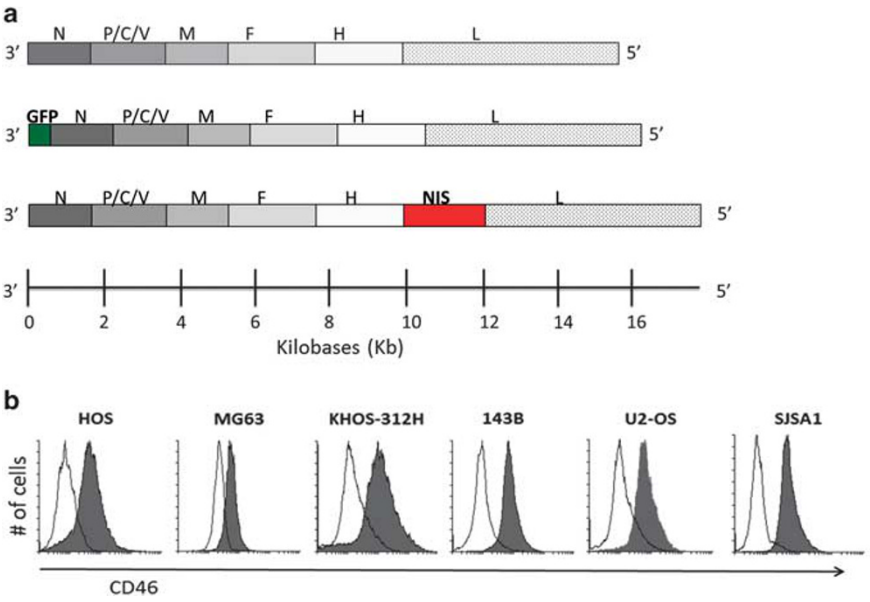

Figure 1. Schematic representation of measles virus genome. (**a**) Genomic organization of MV-Edmonston derivatives, MV-expressing green fluorescent protein (MV-GFP) and MV-expressing sodium iodide symporter (MV-NIS). N, nucleoprotein; P, phosphoprotein; M, matrix protein; F, fusion protein; H, hemagglutinin; L, large protein; GFP, green fluorescent protein; NIS, sodium iodide symporter. Expression of the measles virus CD46 receptor in osteosarcoma lines. (**b**) Osteosarcoma cell lines were tested for the MV receptor CD46, by flow cytometry. Solid line histograms represent isotype control staining, whereas CD46 staining is represented by shaded histograms. CD46 expression was detectable in all cell lines tested.

In this study we demonstrated significant antitumor efficacy of MV derivatives (including MV-NIS and MV-GFP) against OS lines and xenografts. Expression of NIS in MV infected cells resulted in effective tumor cell uptake of 99mTc and F-18 tetrafluoroborate for *in vivo* monitoring of virus infection by SPECT and PET-CT. Moreover, we demonstrated that treatment of athymic nude xenografts with MV-NIS resulted in statistically significant decrease in the growth of orthotopic tumors, and conferred a significant survival advantage in mice bearing orthotopic tibial bone or metastatic pulmonary tumors.

MATERIALS AND METHODS

Cell culture

HOS, MG63, 143B, KHOS-312H, U2OS and SJSA1 OS cell lines were purchased from the American Type Culture Collection (ATCC; Manassas, VA, USA). SJSA1 cells were grown in Roswell Park Memorial Institute medium and all other cells in Dulbecco's modified Eagle's medium supplemented with 10% fetal bovine serum and 1× penicillin–streptomycin. Cells were kept at 37 °C in a humidified atmosphere of 5% CO_2.

MV strains

Construction of MV-GFP and the NIS protein (MV-NIS) has been previously described.[26,29] The viruses were propagated in Vero cells and titrated as previously described.[27]

Determination of CD46 and Nectin-4 expression by flow cytometry

Cells were grown to confluence in T75 flasks, washed with phosphate buffered saline, and harvested in Versene solution (Gibco, Carlsbad, CA, USA). Cells were washed twice with 0.5% bovine serum albumin-phosphate buffered saline, and incubated with FITC conjugated mouse antihuman CD46 antibody (BD Pharmingen, San Jose, CA, USA), PE conjugated mouse antihuman Nectin-4 (R&D Systems, Minneapolis, MN, USA), or the conjugated isotype control antibody for 1 h on ice. Samples were washed twice with 0.5% bovine serum albumin-phosphate buffered saline, fixed in 0.5% paraformaldehyde and run on a Becton–Dickinson FACScan Plus cytometer (San Jose, CA, USA). Flowingsoftware was used for file analysis (Cell Imaging Core, Turku Centre for Biotechnology, Finland).

Cell viability assays

HOS, MG63, 143B, KHOS-312H, U2OS and SJSA1 cells (10 000 cells per well) were seeded in a 96-well plate and infected with the indicated virus on the following day at a multiplicity of infection of 1 and 0.1, in 50 µl of opti-minimal essential medium. On days 1 through 4 after infection, cell viability was measured using the MTS cell proliferation assay (Promega, Madison, WI, USA), following the manufacturer recommendations.

Assessment of viral replication in OS cell lines

OS lines were plated in six-well plates at a density of 4×10^5 per well. Cells were infected at an multiplicity of infection of 1, incubated at 32 °C in a humidified atmosphere of 5% CO_2, and harvested at 1, 3 and 5 days after infection. The viruses were released by two cycles of freeze/thawing, and the viral titer was determined by end point dilution assay and expressed as 50% tissue culture infectious dose ($TCID_{50}$) per ml on Vero cells.

Western blot

Cells were collected in RIPA buffer and samples loaded on 7.5% precast polyacrylamide gel (Bio-Rad, Hercules, CA, USA) for SDS-PAGE. Gel was transferred to polyvinylidene difluoride membrane. Membranes were blocked (5% nonfat milk in Tris-buffered saline–Tween) and incubated with anti-N protein antibody developed in our laboratory (publication pending, Ianko Iankov) overnight at 4 °C. Rabbit mouse-specific polyvalent immunoglobulin (G, A, M) HRP conjugate (diluted 1:2000 in 5% dry milk in phosphate buffered saline) was used as the secondary antibody (Pierce, Rockford, IL, USA). Anti-human β-actin was used as a control to ensure uniform loading. Antibody binding was visualized by enhanced chemiluminescence (Pierce, Rockford, IL, USA).

Animal experiments

143B OS cells were transduced with lentivirus-expressing firefly luciferase (143B-luc). 1×10^6 cells were then injected subcutaneously into the right flank or into the right tibial bone of 5-week old nude mice, as described

elsewhere.[30] For the lung metastasis model, 1×10^6 cells were injected into the tail vein of mice and lung tumors allowed to engraft over 10 days. Mice were considered to have reached the euthanasia endpoint if > 20% weight loss, tumor exceeding 10% of body weight or if their tumors developed ulcerations. All experimental protocols were approved by the Mayo Clinic Institutional Animal Care and Use Committee.

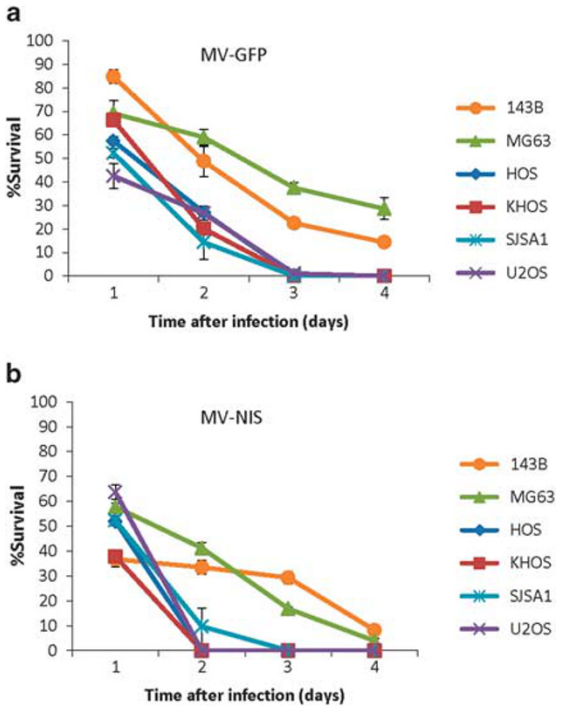

Figure 2. Osteosarcoma (OS) cell lines are susceptible to measles virus (MV) infection. (**a**) Significant cytopathic effect observed against different OS cell lines following MV-expressing green fluorescent protein (MV-GFP) infection at an multiplicity of infection (MOI) of 1 ($n = 3$ independent experiments). (**b**) MV-expressing sodium iodide symporter (MV-NIS) infection at an MOI of 1 similarly led to significant cell death ($n = 3$ independent experiments). The MV-NIS cytopathic effect peaked earlier in the majority of cell lines, likely reflecting the impact of different transgene position on viral replication.

In vivo imaging

Engraftment in tibial bone was verified 4 days post implantation and pulmonary engraftment was verified 10 days post implantation on a Xenogen bioluminescence Imaging System (Waltham, MA, USA). In order to assess viral replication *in vivo*, subcutaneous xenografts were treated intratumorally with MV-NIS every 4 days for 2 weeks. On day 14 mice were injected with ^{99}Tc (100 μCi) intraperitoneally, and tumor imaging was performed serially with a high-resolution micro single-photon emission computed tomography (SPECT) system (X-SPECT; Gamma Medica-Ideas, Northridge, CA, USA).

Dynamic PET imaging was performed in intravenously treated orthotopic xenografts on day 14 of MV-NIS therapy. Following intraperitoneal injection of 0.07 MBq Na [^{18}F]BF_4 per gr of weight, animal PET scans were acquired for 60 min followed by an X-ray scan using the GENISYS4 PET imaging system (Sofie Biosciences, Culver City, CA, USA). The images were analyzed for standardized uptake value in tumor, stomach, thyroid and bladder using AMIDE image analysis tool (Stanford University, Stanford, CA, USA). Na [^{18}F]BF_4 was prepared by a modification of Jauregui-Osoro *et al.*[28] Isotope exchange performed in 0.5 M HCl at 130 °C for 10 min followed by neutralization on a Dionex OnGuard AG SPE cartridge (Atlanta, GA, USA) and fluoride separation on two Waters neutral alumina SPE cartridges (Milford, MA, USA). The product was then sterile filtered through a 0.2 μ filter and radiochemical purity was > 99% by silica gel thin-layer chromatography (MeOH). The specific activity was 2–5 μCi μg^{-1}.

Statistical analyses

Data were analyzed using GraphPad Prism (GraphPad software, San Diego, CA, USA).

RESULTS

MV-GFP and MV-NIS have potent anti-tumor activity against OS cell lines *in vitro*

We used two trackable oncolytic MV-Edm derivatives in our *in vitro* studies (Figure 1a): MV-GFP, expressing the green fluorescence protein, and MV-NIS. A panel of six OS cell lines were studied and all of them expressed high levels of the MV receptor, CD46 (Figure 1b). Cell lines were also analyzed for expression of Nectin-4, the epithelial receptor for MV and no significant expression was detected (data not shown).

Following infection with MV-GFP at an multiplicity of infection of 1 there was efficient killing of four of six OS cell line monolayers (U2OS, HOS, KHOS-312H and SJSA1 cells) within 48–72 h (Figure 2a). MV-NIS had superior *in vitro* efficacy as compared with MV-GFP, with activity against all six lines, including the MG63 and 143B cells (Figure 2b). Because of the transcriptional gradient

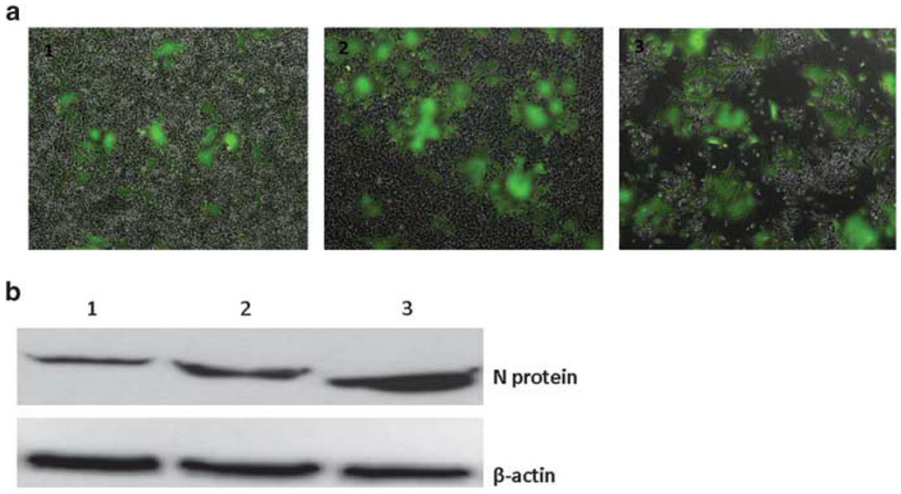

Figure 3. Measles virus-expressing green fluorescent protein (MV-GFP) infection kinetics in the moderately susceptible 143B sarcoma cell line. MV-GFP infection leads to (**a**) GFP expression is increased over time until monolayer obliteration. Images A1, 2 and 3 were taken on days 1, 2 and 3, respectively following infection (4× magnification). (**b**) Increased expression of measles N protein during the same time course.

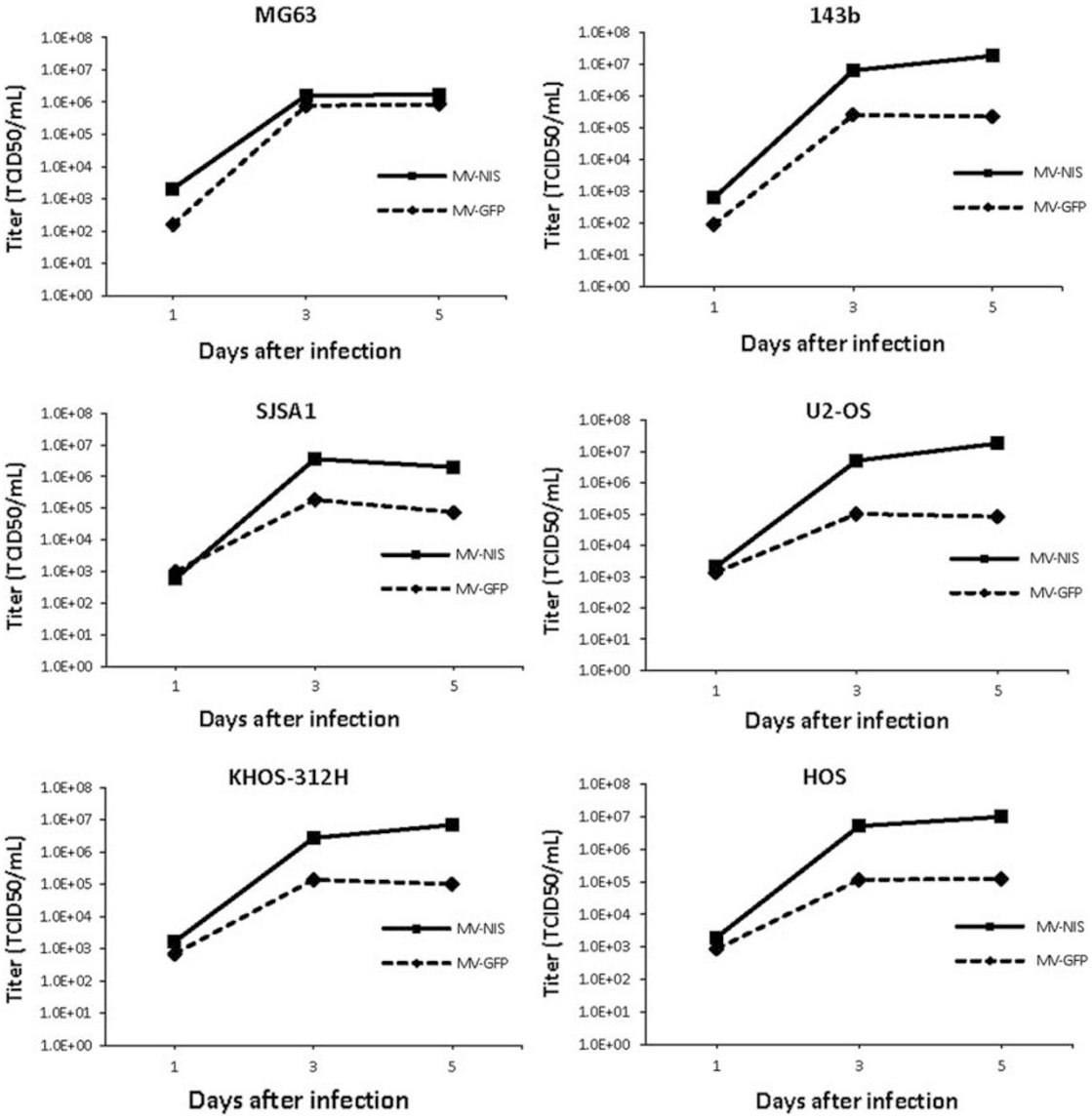

Figure 4. Measles virus-expressing green fluorescent protein (MV-GFP) and MV-expressing sodium iodide symporter (MV-NIS) replicate efficiently in tumor lines, as demonstrated by one-step viral growth curves. Increased replication of MV-NIS as compared with MV-GFP was seen in the panel of six osteosarcoma cell lines.

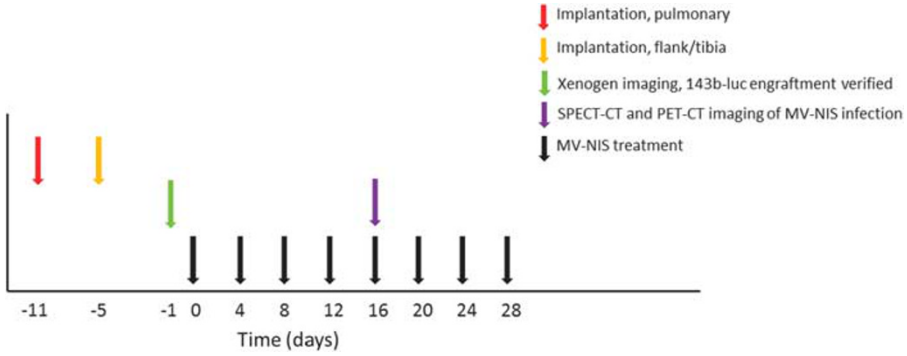

Figure 5. Measles virus-expressing sodium iodide symporter (MV-NIS) treatment schema. 143B-luc osteosarcoma cells were implanted into the right flank, right tibial bone or via tail vein injection (lung metastasis model). On the day prior to the MV-NIS treatment initiation, engraftment was confirmed by Xenogen bioluminescence imaging. Mice were then randomized to receive intravenous MV-NIS treatment or heat-inactivated virus every 4 days for a total of 4 weeks. Two weeks after the initiation of therapy, mice were also imaged by single photon emission computed tomography or positron emission tomography–computed tomography to monitor *in vivo* viral activity.

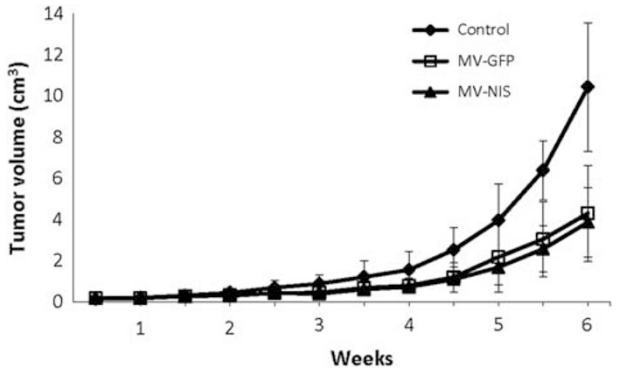

Figure 6. Flank tumor growth was suppressed by intratumoral (IT) therapy with oncolytic measles virus strains. Osteosarcoma flank xenografts were treated every 4 days with IT injections of 1×10^6 $TCID_{50}$ MV expressing green fluorescent protein (MV-GFP), MV-NIS or heat-inactivated control virus ($n = 5$ per group), which led to suppression of tumor growth both in MV-GFP-($P = 0.0407$) and MV-NIS-($P = 0.0374$) treated mice.

during MV replication[31] the different transgene positions within the MV genome (position one for MV-GFP vs position six for MV-NIS) could explain the difference in the cytopathic effect we observed between the two strains.

Though the pulmonary metastatic 143B cell line was intermediately susceptible to MV-GFP oncolysis, infection with MV-GFP led to abundant GFP expression. Green fluorescence increased over the course of infection and syncytia grew in size and number ultimately leading to eradication of the monolayer. MV nucleoprotein (N-protein) expression was verified by western blot and N-protein expression increased over the first 3 days of infection (Figures 3a and b). Relative resistance to infection of 143B cells to MV-GFP could be overcome by increasing the multiplicity of infection (data not shown). In one step viral growth curves both strains resulted in replication, although higher titers of MV-NIS vs MV-GFP were obtained (Figure 4).

Characterization of 143B-luc flank, orthotopic and metastatic OS xenograft models

To investigate the therapeutic potential of MV-NIS treatment in the recurrent or pulmonary metastatic setting the aggressive and highly metastatic 143B cell line was chosen for xenograft development. 143B cells were transduced by a lentivirus-expressing firefly luciferase, to generate 143B-luc cells. We injected 100 µl of 143B-luc tumor cells (1×10^6) into the right flank, right tibial bone or intravenously into the tail vein of 5 week old mice to establish xenografts. Following verification of engraftment mice were then treated either with MV-NIS or heat-inactivated control virus every 4 days for a total of 4 weeks (Figure 5). Subcutaneous and orthotopic tibial tumors could be detected by luciferin bioluminescence within 4 days of implantation. Lung engraftment was similarly verified at 10 days post intravenous (IV) implantation (Supplementary Figure).

MV-NIS has potent antitumor activity in mouse xenografts

Flank tumors were generated, and were treated every four days with intratumoral (IT) injections of 1×10^6 $TCID_{50}$ MV-GFP, MV-NIS or heat-inactivated control virus ($n = 5$ per group) (similar to the schema of Figure 5) and tumor size was measured with digital calipers. A decrease in tumor growth was observed (Figure 6) with MV-GFP ($P = 0.0407$) and MV-NIS treatment ($P = 0.0374$).

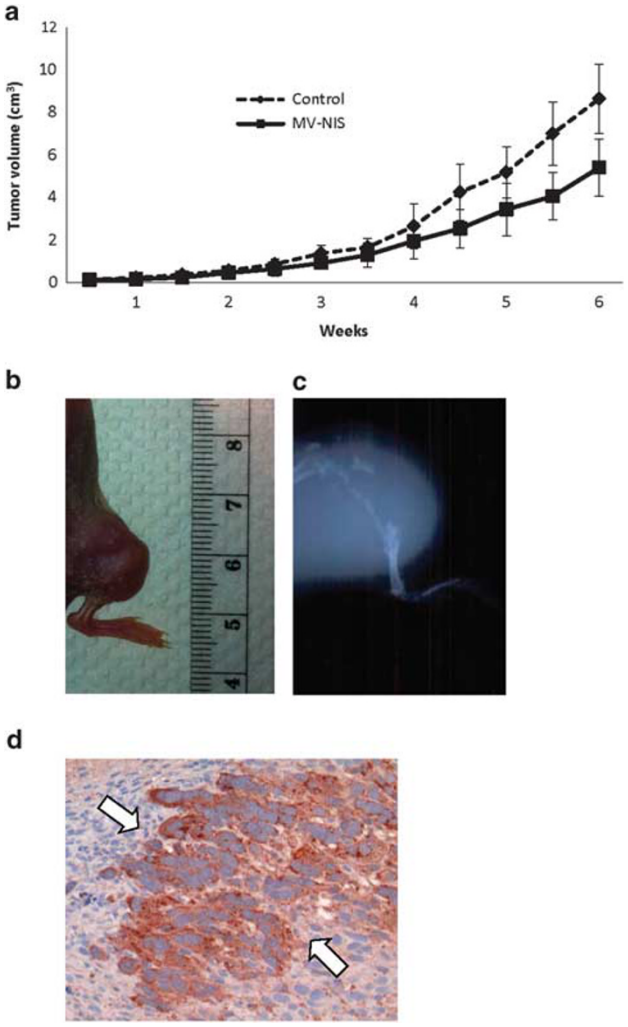

Figure 7. Systemic measles virus-expressing sodium iodide symporter (MV-NIS) therapy results in antitumor activity in orthotopic xenografts. Orthotopic tumors were treated every 4 days with intravenous injections of 1×10^6 $TCID_{50}$ MV-NIS or heat-inactivated control virus ($n = 10$ per group). (**a**) MV-NIS treatment suppressed the the growth of leg tumors compared with controls ($P = 0.0014$), data are shown as mean ± s.e., $n = 10$ per group. A representative photograph of (**b**) an orthotopic tibial tumor 2 weeks after implantation and (**c**) representative radiographic image of an orthotopic leg tumor 6 weeks after engraftment is shown. (**d**) After 2 weeks of MV-NIS therapy excised orthotopic tibial tumors show evidence of syncytia formation and expression of measles N-protein by immunohistochemistry.

In the orthotopic model, tibial bone tumors grew rapidly in heat-inactivated virus-treated animals ($n = 10$) and in some cases tumors were associated with lytic destruction of the underlying tibial bone (Figures 7b and c). IV treatment with MV-NIS ($n = 10$) led to a significant decrease in the growth of orthotopic leg tumors, $P = 0.0014$; data shown as mean ± s.e. (Figure 7a). After 2 weeks of MV therapy, there was clear evidence of syncytial formation with nuclear coalescence and positive staining for the viral N-protein (Figure 7d) in MV-treated tumors. Metastatic tumor foci were often noted post mortem; the majority of metastases were involving the lungs with metastatic involvement of appendicular and axial bony skeleton also being common. Mice with pulmonary tumors generally had to be euthanized due to cachexia, lethargy, hunched posture and in some instances cord

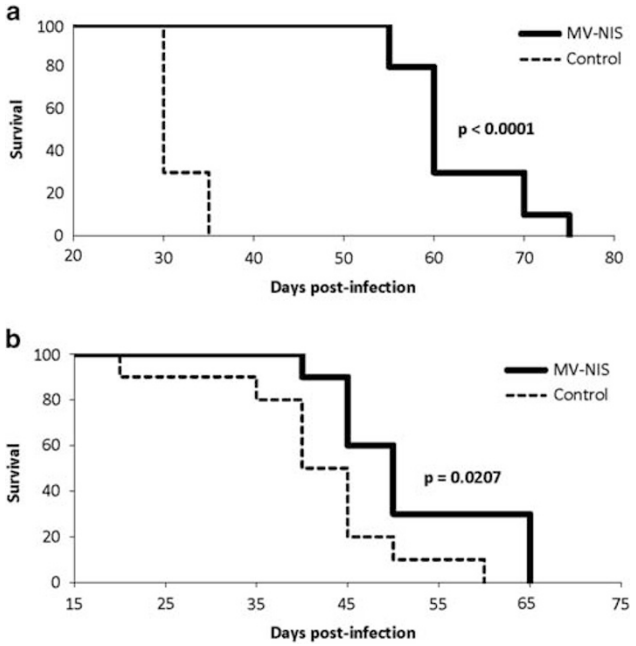

Figure 8. Therapy with measles virus-expressing sodium iodide symporter (MV-NIS) administered systemically, increases survival in osteosarcoma xenograft models. MV-NIS treatment was associated with a significant increase in overall survival in (**a**) the tibial orthotopic ($P < 0.0001$) and (**b**) pulmonary metastatic ($P = 0.0207$) models as shown by Kaplan–Meier curves comparing control with MV-NIS treatment twice weekly for 4 weeks, $n = 10$ per treatment group.

compression and hind limb paralysis secondary to metastatic involvement of the vertebral spine.

We also assessed survival following intravenous MV-treatment both in tibial orthotopic and pulmonary metastatic OS xenografts. Xenografts treated every 4 days with MV-NIS ($n = 10$) at a dose of 1×10^6 $TCID_{50}$ had a statistically significant prolongation of survival compared with mice treated with heat-inactivated virus ($n = 10$) both in the orthotopic tibial bone model ($P < 0.0001$, Figure 8a) and the pulmonary metastatic model ($P = 0.0207$, Figure 8b). In the orthotopic model, median survival of the treated mice was 60 days compared with 30 days for control animals. In fact, all MV-NIS-treated mice with orthotopic tibial xenografts were alive on day 40, as compared with none of the mice in the control group.

MV-NIS infects OS xenografts and NIS transgene expression can be monitored *in vivo*

In a separate study in order to assess viral replication *in vivo*, mice were treated with MV-NIS every 4 days for 2 weeks either directly into flank tumors or intravenously in established orthotopic xenografts. Monitoring of viral infection and replication *in vivo* was then performed using two different imaging modalities. In the subcutaneous flank tumor model MV-NIS-treated mice (IT injection) were administered Tc-99m into the peritoneum (IP) on day 14 and then imaged 30 min later by CT-SPECT. IT accumulation of Tc-99m in subcutaneous flank tumors was seen in mice treated with MV-NIS (Figure 9a), but not in animals treated with the inactive virus preparation (Figure 9a, lower panel). Cross-sectional imaging demonstrated MV-NIS gene expression in tumors; expression of NIS by infected tumor cells resulted in Tc-99m concentration, which we could detect by SPECT imaging.

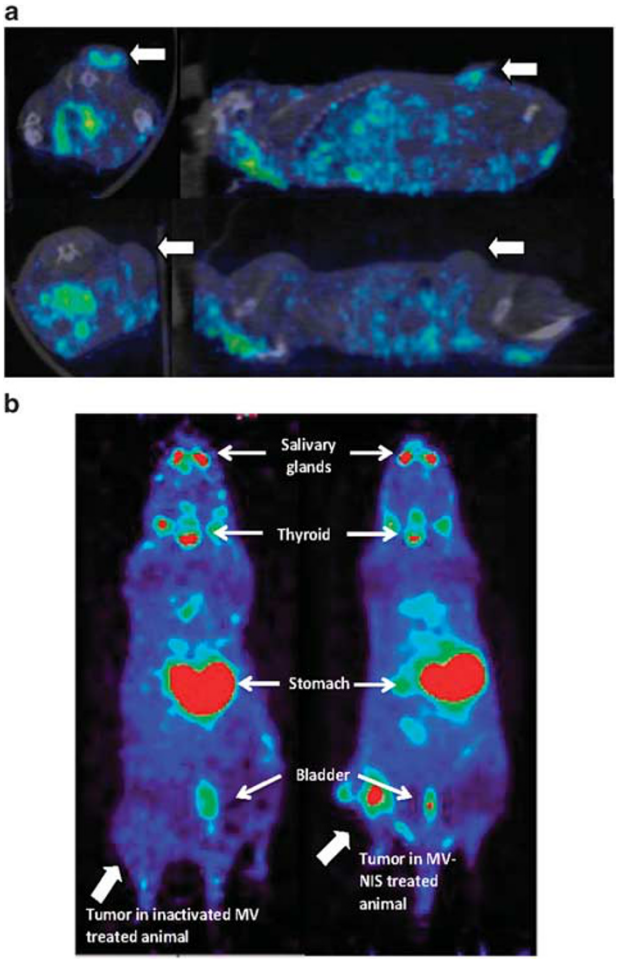

Figure 9. Measles virus-expressing sodium iodide symporter (MV-NIS) treatment allows real-time *in vivo* imaging of viral replication. After 2 weeks of MV-NIS therapy osteosarcoma xenografts were imaged by single photon emission computed tomography (SPECT) or positron emission tomography–computed tomography (PET-CT). (**a**) Flank xenografts treated every 4 days for 2 weeks with intratumoral injections of 1×10^6 $TCID_{50}$ were imaged by SPECT. Representative image shows uptake of Tc-99m in flank tumors (large arrows) of MV-NIS-treated (9A, upper panel), but not inactivated virus-treated animals (9A, lower panel). (**b**) Orthotopic tibial xenografts were treated intravenously every 4 days for 2 weeks with 1×10^6 $TCID_{50}$ MV-NIS. They were subsequently imaged by PET-CT after F-18 tetrafluoroborate administration. In contrast to MV-NIS-treated animals (9B, right panel), no significant uptake was seen in control virus-treated mice (9B, left panel).

We next evaluated the ability of IV MV-NIS therapy to result in the IT concentration of the radioactive tracer [^{18}F] tetrafluoroborate, through NIS mediated transport. PET-CT imaging performed 60 min after IP administration F-18 tetrafluoroborate resulted in significant uptake in tibial tumors (Figure 9b) and thereby convincingly demonstrated viral gene expression in OS tumors following systemic viral administration.

DISCUSSION

OS is an aggressive bone cancer with peak incidence in childhood, adolescence and early adulthood. Although surgical advancements and combination chemotherapy have led to a 65–70% cure rate, no additional improvement in survival

has materialized during the last two decades; new therapeutic approaches are urgently needed for this young patient population.

Oncolytic measles virotherapy provides a novel and safe therapeutic strategy for treatment of recurrent and metastatic OS. The fact that viruses have adapted over millennia of evolution to efficiently invade cells and overtake their biosynthetic machinery, makes them attractive candidates for the development of novel antitumor approaches. Other groups have used replication-competent oncolytic viruses in the treatment of OS mostly focusing on *in vitro* efficacy studies and loco-regional *in vivo* delivery. Oncolytic Semliki forest virus was previously shown to have *in vitro* activity, and IT injections in an orthotopic K7M3 tumor model showed tumor regression and survival benefit. Poliovirus targets the cell surface receptor CD155, and was found to induce apoptosis through induction of caspases 7 and 3 in bone and soft tissue sarcoma cells.[32] Vesicular stomatitis virus delivered by isolated limb perfusion has similarly been shown to suppress osteosarcoma growth in an immune competent rat model.[30] Our study represents the first report that demonstrates efficacy of an engineered MV strain in treatment of bone sarcomas, following both IT and systemic administration in challenging to treat orthotopic and lung metastatic models.

In this study, we have demonstrated that MV infects OS cell lines and that replication of MV is efficient, with evidence of viral replication to high titers in OS cells. Indeed, IV delivery of MV-NIS resulted in a decrease in growth of 143B orthotopic tumors and prolongation of survival of tumor bearing mice. We have also shown that SPECT or PET-CT allow for efficient tracking of infected OS cells *in vivo*. We showed that IT and IV therapy can both be monitored *in vivo*, and that SPECT and PET-CT imaging are sensitive enough to differentiate infected tumor cell uptake. The ability to monitor viral replication and transgene expression *in vivo* also allows for pharmacodynamic measurements of viral distribution and dissemination, and various radioactive substrates can be used to quantify NIS gene expression including ^{123}I, F-18 tetrafluoroborate and 99mTc. Recently reported clinical data support that SPECT-CT can be used to monitor viral replication in patients, for example, myeloma tumor deposits following systemic administration.[15] NIS may also be used as a therapeutic transgene capable of further increasing the oncolytic potency of MV-NIS by allowing the intracellular concentration of radioisotopes, such as the beta particle emitter, ^{131}I as a mediator of radiovirotherapy.[33]

Infection with oncolytic MV has also been shown to directly activate the immune system in immune competent preclinical models. The viral hemagglutinin has been shown to interact with and induce toll-like receptor-2 (TLR-2) signaling, and TLR-7 and TLR-9 have also been shown to be involved in viral nucleic acid detection and antiviral signaling.[34,35] Similarly, in preclinical studies MV vaccine-infected tumor cells cocultured with plasmacytoid dendritic cells induce maturation of dendritic cells into efficient antigen-presenting cells, with upregulation of costimulatory molecules CD40 and CD86.[36] The antitumor activity of DCs depend on interferon-α (IFN-α)-mediated autocrine stimulation and IFN-α can also directly stimulate apoptosis in tumor cells.[37] IFN-α induction by 2-methoxyestradiol in OS cells has similarly been shown to have antiproliferative effects *in vitro*.[38] MV-Edm derivatives have also been engineered to express immunostimulatory cytokines including granulocyte-macrophage colony stimulating factor (MV-GM-CSF) and IFNβ (MV-IFNβ)[39,40]. both important immune regulators that have been shown to induce antitumor immune responses in several tumor types.[41,42] Work in our laboratory has also demonstrated that MV engineering to express the immunomodulatory *Helicobacter pylori* neutrophil-activating protein induces a brisk Th1 cytokine response *in vivo*, associated with high levels of TNF-α production as well as prolongation of survival in an aggressive model of lung metastatic breast cancer.[43] These engineered strains could also have excellent applicability in the treatment of OS as they could bridge oncolytic virotherapy with sarcoma immunotherapy, and they are currently in preclinical investigation.

MV has a proven record of safety in large-scale immunization campaigns; however, widespread immunization in the Western world can also pose a major challenge to oncolytic measles virotherapy approaches. Although delivery challenges are difficult to address in immunocompromised xenograft models, several techniques have been used to augment treatment efficacy. Rapid clearance of virus can take place shortly after the virus is introduced into an immunized host and represents a potential limitation for systemic administration approaches. Strategies for augmenting potency and ensuring safety of virotherapy include viral genetic manipulations, as already described, concurrent chemotherapy and immunomodulatory use of cyclophosphamide as has been demonstrated for MV-NIS in primate models.[44] IV delivery of high doses of MV in patients lacking anti-MV-neutralizing antibodies has been successfully employed against refractory multiple myeloma.[15] However, in the presence of neutralizing titers of anti-measles antibodies infected cell carriers have been used efficaciously to deliver MV to tumor cells;[45] the infected cell carriers can circumvent and increase efficacy in the setting of pre-existing anti-measles humoral immunity. This concept has been demonstrated by employing dendritic cells in breast cancer xenografts[11] and mesenchymal stem cell carriers in passively immunized mice bearing ovarian xenografts.[46] More recently, human bone marrow-derived mesenchymal stromal cell carriers were similarly used in passively immunized mice to efficiently deliver MV in a systemic xenograft model of precursor B-lineage-acute lymphoblastic leukemia.[47]

In summary, our results demonstrate that MV-NIS exhibits significant therapeutic effect against human OS cell lines *in vitro* and orthotopic and metastatic disease models *in vivo*. MV could provide a new therapeutic addition to multimodality treatment of patients with recurrent or metastatic OS, especially given the lack of cross-resistance with existing therapies and continuing improvements in the production of high titer therapeutic viral preparations. Promising emerging data in other tumor types such as ovarian cancer[10] and multiple myeloma[15] further highlight this potential. Based on these encouraging results, this approach has significant translational potential, and further preclinical and clinical studies are warranted.

CONFLICT OF INTEREST

The authors declare no conflict of interest.

ACKNOWLEDGEMENTS

We thank Ianko Iankov, MD, PhD for his methodological assistance and kindly providing the anti MV nucleoprotein antibody used in this study. We also thank Mark Federspiel, PhD and the Viral Vector Production Laboratory (Mayo Clinic) for providing MV-NIS preparations used in our studies and Hirosha Geekiyanage, PhD for technical advice and helpful discussions. Support for this research provided by the Clinical Investigator Training Program and a small grant from the Department of Oncology, Mayo Clinic; and NCI/NIH grants R01CA 154348 and R01CA 136547.

REFERENCES

1 Skubitz KM, D'Adamo DR. Sarcoma. *Mayo Clin Proc* 2007; **82**: 1409–1432.
2 Link MP, Goorin AM, Miser AW, Green AA, Pratt CB, Belasco JB *et al.* The effect of adjuvant chemotherapy on relapse-free survival in patients with osteosarcoma of the extremity. *N Engl J Med* 1986; **314**: 1600–1606.
3 Provisor AJ, Ettinger LJ, Nachman JB, Krailo MD, Makley JT, Yunis EJ *et al.* Treatment of nonmetastatic osteosarcoma of the extremity with preoperative and postoperative chemotherapy: a report from the Children's Cancer Group. *J Clin Oncol* 1997; **15**: 76–84.
4 Ritter J, Bielack SS. Osteosarcoma. *Ann Oncol* 2010; **21**(Suppl 7): vii320–vii325.

5 Msaouel P, Opyrchal M, Domingo Musibay E, Galanis E. Oncolytic measles virus strains as novel anticancer agents. *Expert Opin Biol Ther* 2013; **13**: 483–502.
6 Bluming AZ, Ziegler JL. Regression of Burkitt's lymphoma in association with measles infection. *Lancet* 1971; **2**: 105–106.
7 Taqi AM, Abdurrahman MB, Yakubu AM, Fleming AF. Regression of Hodgkin's disease after measles. *Lancet* 1981; **1**: 1112.
8 Cutts FT, Markowitz LE. Successes and failures in measles control. *J Infect Dis* 1994; **170**(Suppl 1): S32–S41.
9 Allen C, Paraskevakou G, Liu C, Iankov ID, Msaouel P, Zollman P *et al.* Oncolytic measles virus strains in the treatment of gliomas. *Expert Opin Biol Ther* 2008; **8**: 213–220.
10 Galanis E, Hartmann LC, Cliby WA, Long HJ, Peethambaram PP, Barrette BA *et al.* Phase I trial of intraperitoneal administration of an oncolytic measles virus strain engineered to express carcinoembryonic antigen for recurrent ovarian cancer. *Cancer Res* 2010; **70**: 875–882.
11 Iankov ID, Msaouel P, Allen C, Federspiel MJ, Bulur PA, Dietz AB *et al.* Demonstration of anti-tumor activity of oncolytic measles virus strains in a malignant pleural effusion breast cancer model. *Breast Cancer Res Treat* 2010; **122**: 745–754.
12 Liu C, Sarkaria JN, Petell CA, Paraskevakou G, Zollman PJ, Schroeder M *et al.* Combination of measles virus virotherapy and radiation therapy has synergistic activity in the treatment of glioblastoma multiforme. *Clin Cancer Res* 2007; **13**: 7155–7165.
13 Myers R, Harvey M, Kaufmann TJ, Greiner SM, Krempski JW, Raffel C *et al.* Toxicology study of repeat intracerebral administration of a measles virus derivative producing carcinoembryonic antigen in rhesus macaques in support of a phase I/II clinical trial for patients with recurrent gliomas. *Hum Gene Ther* 2008; **19**: 690–698.
14 Pavlos M, Ianko DI, Cory A, John CM, Veronika von M, Roberto C *et al.* Engineered measles virus as a novel oncolytic therapy against prostate cancer. *The Prostate* 2009; **69**: 82–91.
15 Russell SJ, Federspiel MJ, Peng KW, Tong C, Dingli D, Morice WG *et al.* Remission of disseminated cancer after systemic oncolytic virotherapy. *Mayo Clin Proc* 2014; **89**: 926–933.
16 Naniche D, Varior-Krishnan G, Cervoni F, Wild TF, Rossi B, Rabourdin-Combe C *et al.* Human membrane cofactor protein (CD46) acts as a cellular receptor for measles virus. *J Virol* 1993; **67**: 6025–6032.
17 Muhlebach MD, Mateo M, Sinn PL, Prufer S, Uhlig KM, Leonard VH *et al.* Adherens junction protein nectin-4 is the epithelial receptor for measles virus. *Nature* 2011; **480**: 530–533.
18 Dorig RE, Marcil A, Chopra A, Richardson CD. The human CD46 molecule is a receptor for measles virus (Edmonston strain). *Cell* 1993; **75**: 295–305.
19 Mateo M, Navaratnarajah CK, Syed S, Cattaneo R. The measles virus hemagglutinin beta-propeller head beta4-beta5 hydrophobic groove governs functional interactions with nectin-4 and CD46 but not with the signaling lymphocytic activation molecule. *J Virol* 2013; **87**: 9208–9216.
20 Jurianz K, Ziegler S, Garcia-Schuler H, Kraus S, Bohana-Kashtan O, Fishelson Z *et al.* Complement resistance of tumor cells: basal and induced mechanisms. *Mol Immunol* 1999; **36**: 929–939.
21 Surowiak P, Materna V, Maciejczyk A, Kaplenko I, Spaczynski M, Dietel M *et al.* CD46 expression is indicative of shorter revival-free survival for ovarian cancer patients. *Anticancer Res* 2006; **26**: 4943–4948.
22 Allen C, Vongpunsawad S, Nakamura T, James CD, Schroeder M, Cattaneo R *et al.* Retargeted oncolytic measles strains entering via the EGFRvIII receptor maintain significant antitumor activity against gliomas with increased tumor specificity. *Cancer Res* 2006; **66**: 11840–11850.
23 Bello MJ, de Campos JM, Kusak ME, Vaquero J, Sarasa JL, Pestana A *et al.* Molecular analysis of genomic abnormalities in human gliomas. *Cancer Genet Cytogenet* 1994; **73**: 122–129.
24 Linge C, Gewert D, Rossmann C, Bishop JA, Crowe JS. Interferon system defects in human malignant melanoma. *Cancer Res* 1995; **55**: 4099–4104.
25 Ahn BC. Sodium iodide symporter for nuclear molecular imaging and gene therapy: from bedside to bench and back. *Theranostics* 2012; **2**: 392–402.
26 Dingli D, Peng KW, Harvey ME, Greipp PR, O'Connor MK, Cattaneo R *et al.* Image-guided radiovirotherapy for multiple myeloma using a recombinant measles virus expressing the thyroidal sodium iodide symporter. *Blood* 2004; **103**: 1641–1646.
27 Msaouel P, Iankov ID, Allen C, Aderca I, Federspiel MJ, Tindall DJ *et al.* Noninvasive imaging and radiovirotherapy of prostate cancer using an oncolytic measles virus expressing the sodium iodide symporter. *Mol Ther* 2009; **17**: 2041–2048.
28 Jauregui-Osoro M, Sunassee K, Weeks AJ, Berry DJ, Paul RL, Cleij M *et al.* Synthesis and biological evaluation of [(18)F]tetrafluoroborate: a PET imaging agent for thyroid disease and reporter gene imaging of the sodium/iodide symporter. *Eur J Nucl Med Mol Imaging* 2010; **37**: 2108–2116.
29 Duprex WP, McQuaid S, Hangartner L, Billeter MA, Rima BK. Observation of measles virus cell-to-cell spread in astrocytoma cells by using a green fluorescent protein-expressing recombinant virus. *J Virol* 1999; **73**: 9568–9575.
30 Kubo T, Shimose S, Matsuo T, Fujimori J, Sakaguchi T, Yamaki M *et al.* Oncolytic vesicular stomatitis virus administered by isolated limb perfusion suppresses osteosarcoma growth. *J Orthop Res* 2011; **29**: 795–800.
31 Conzelmann KK. Nonsegmented negative-strand RNA viruses: genetics and manipulation of viral genomes. *Annu Rev Genet* 1998; **32**: 123–162.
32 Atsumi S, Matsumine A, Toyoda H, Niimi R, Iino T, Nakamura T *et al.* Oncolytic virotherapy for human bone and soft tissue sarcomas using live attenuated poliovirus. *Int J Oncol* 2012; **41**: 893–902.
33 Penheiter AR, Russell SJ, Carlson SK. The sodium iodide symporter (NIS) as an imaging reporter for gene, viral, and cell-based therapies. *Curr Gene Ther* 2012; **12**: 33–47.
34 Kumar H, Kawai T, Akira S. Toll-like receptors and innate immunity. *Biochem Biophys Res Commun* 2009; **388**: 621–625.
35 Gilliet M, Cao W, Liu YJ. Plasmacytoid dendritic cells: sensing nucleic acids in viral infection and autoimmune diseases. *Nat Rev Immunol* 2008; **8**: 594–606.
36 Guillerme JB, Boisgerault N, Roulois D, Menager J, Combredet C, Tangy F *et al.* Measles virus vaccine-infected tumor cells induce tumor antigen cross-presentation by human plasmacytoid dendritic cells. *Clin Cancer Res* 2013; **19**: 1147–1158.
37 Thyrell L, Erickson S, Zhivotovsky B, Pokrovskaja K, Sangfelt O, Castro J *et al.* Mechanisms of Interferon-alpha induced apoptosis in malignant cells. *Oncogene* 2002; **21**: 1251–1262.
38 Wimbauer F, Yang C, Shogren KL, Zhang M, Goyal R, Riester SM *et al.* Regulation of interferon pathway in 2-methoxyestradiol-treated osteosarcoma cells. *BMC Cancer* 2012; **12**: 93.
39 Grote D, Cattaneo R, Fielding AK. Neutrophils contribute to the measles virus-induced antitumor effect: enhancement by granulocyte macrophage colony-stimulating factor expression. *Cancer Res* 2003; **63**: 6463–6468.
40 Li H, Peng KW, Dingli D, Kratzke RA, Russell SJ. Oncolytic measles viruses encoding interferon beta and the thyroidal sodium iodide symporter gene for mesothelioma virotherapy. *Cancer Gene Ther* 2010; **17**: 550–558.
41 Gupta R, Emens LA. GM-CSF-secreting vaccines for solid tumors: moving forward. *Discov Med* 2010; **10**: 52–60.
42 Bracarda S, Eggermont AM, Samuelsson J. Redefining the role of interferon in the treatment of malignant diseases. *Eur J Cancer* 2010; **46**: 284–297.
43 Iankov ID, Allen C, Federspiel MJ, Myers RM, Peng KW, Ingle JN *et al.* Expression of immunomodulatory neutrophil-activating protein of *Helicobacter pylori* enhances the antitumor activity of oncolytic measles virus. *Mol Ther* 2012; **20**: 1139–1147.
44 Myers RM, Greiner SM, Harvey ME, Griesmann G, Kuffel MJ, Buhrow SA *et al.* Preclinical pharmacology and toxicology of intravenous MV-NIS, an oncolytic measles virus administered with or without cyclophosphamide. *Clin Pharmacol Ther* 2007; **82**: 700–710.
45 Iankov ID, Blechacz B, Liu C, Schmeckpeper JD, Tarara JE, Federspiel MJ *et al.* Infected cell carriers: a new strategy for systemic delivery of oncolytic measles viruses in cancer virotherapy. *Mol Ther* 2007; **15**: 114–122.
46 Mader EK, Maeyama Y, Lin Y, Butler GW, Russell HM, Galanis E *et al.* Mesenchymal stem cell carriers protect oncolytic measles viruses from antibody neutralization in an orthotopic ovarian cancer therapy model. *Clin Cancer Res* 2009; **15**: 7246–7255.
47 Castleton A, Dey A, Beaton B, Patel B, Aucher A, Davis DM *et al.* Human mesenchymal stromal cells deliver systemic oncolytic measles virus to treat acute lymphoblastic leukemia in the presence of humoral immunity. *Blood* 2014; **123**: 1327–1335.

Supplementary Information accompanies the paper on Cancer Gene Therapy website (http://www.nature.com/cgt)